UV-based technologies for marine water disinfection and the application to ballast water: Does salinity interfere with disinfection processes?

Javier Moreno-Andrés, Leonardo Romero-Martínez, Asunción Acevedo-Merino and Enrique Nebot

Department of Environmental Technologies. Faculty of Marine and Environmental Sciences. CACYTMAR. Campus Universitario Puerto Real, Avda. República Saharaui s/n; 11510 - Puerto Real. Cádiz. Spain.

*Corresponding Author. Javier Moreno-Andrés.
E-mail address: javier.moreno@uca.es (J. Moreno)

Abstract:

Water contained on ships is employed in the majority of activities on a vessel; therefore, it is necessary to correctly manage through marine water treatments. Among the main water streams generated on vessels, ballast water appears to be an emerging global challenge (especially on cargo ships) due to the transport of invasive species and the significant impact that the ballast water discharge could have on ecosystems and human activities. To avoid this problem, ballast water treatment must be implemented prior to water discharge in accordance with the upcoming Ballast Water Management Convention. Different UV-based treatments (photolytic: UV-C and UV/H_2O_2, photocatalytic: UV/TiO_2), have been compared for seawater disinfection. *E. faecalis* is proposed as a biodosimeter organism for UV-based treatments and demonstrates good properties for being considered as a Standard Test Organism for seawater. Inactivation rates by means of the UV-based treatments were obtained using a flow-through UV-reactor. Based on the two variables responses that were studied (kinetic rate constant and UV-Dose reductions), both advanced oxidation processes (UV/H_2O_2 and photocatalysis) were more effective than UV-C treatment. Evaluation of salinity on the processes suggests different responses according to the treatments: major interference on photocatalysis treatment and minimal impact on UV/H_2O_2.

Key Words

E. faecalis, UV-based treatments, Seawater disinfection, Salinity interference, UV-Dose, Ballast water

1. Introduction

Shipping transport moves approximately 90% of the world´s overseas trade (Globallast, 2016). Additionally, the cruise tourism industry has experienced an upturn in recent years: the number of people who have decided to spend their holidays aboard a cruise ship has multiplied fourfold over the last two decades (Cruise Market Watch, 2014). Water on these ships is used for almost all activities performed on board, and it implies the need to also discharge various types of water, which could result in environmental distress. This pressure could be enough to constitute a health hazard to ecosystems and increase marine pollution.

Among the primary water streams generated on vessels, the ballast water emerges as a challenge. This water is needed on oceangoing vessels to ensure ship stability and buoyancy. When it is released into far ecosystems, the organisms contained therein could spread into the new environment resulting in ecological threats and an enormous impact on human activities (Werschkun et al., 2014). Hence, invasive aquatic species in which ballast water is the main vector create a global challenge and one of the most severe pollution problems faced by the world´s oceans (Ojaveer et al., 2014; Werschkun et al., 2014).

It is essential to develop management strategies that include ballast water treatments (BWTs) in order to minimize the spread of organisms in ballast water. Therefore, the International Maritime Organization (IMO) published the International Ballast Water Management Convention (BWMC) (IMO, 2004) which will enter into force in 2017 after having been ratified by 52 contracting parties and carry the shipping tonnage to the treaty to 35.1441% (Globallast, 2016). It will be one of the most significant global steps towards the control of alien aquatic species. There are currently only 2410 ships equipped with BWTs (IMO, 2015) with various configurations, the most frequent being a combination of a filtration step followed by a chemical disinfection phase (Lloyd´s Register, 2014).

In order to achieve the implementation of sustainable practices (environmentally friendly and cost-effective) that reduce the use of chemicals and the consequent harmful by-products formation (Rivas-Hermann et al., 2015; Werschkun et al., 2012), the study of different technologies is increasing. Accordingly, this study is focused on ultraviolet

(UV) based technologies since UV-light "can be considered as a traceless and *green* reagent" (Su et al., 2014).

UV technology is based on light absorption by an organic molecule (Su et al., 2014) as DNA; thus, its application is well-known as a disinfection treatment (Hijnen et al., 2006). Under UV irradiation, several catalysts or oxidants can be photo-activated resulting in an Advanced Oxidation Process (AOP) which uses powerful oxidizing radicals (mostly ·OH) that instantaneously react with microorganisms in water such as bacteria, microalgae, etc. (Gligorovski et al., 2015).

AOPs continue to be a subject of scientific interest in water treatment processes for avoiding specific active substances that are associated with chemical hazards (Čulin and Mustać, 2015; Werschkun et al., 2014). This study is focused on two different AOPs: TiO_2-photocatalysis and UV/H_2O_2. Photocatalysis generates ·OH through light incidence of a semiconductor. It has the advantage of no added chemicals when the catalyst is fixed on the reactor (Chong et al., 2010) which shows great potential as sustainable treatment technology. In the case of the UV/H_2O_2 process, the generation of ·OH is derived by photolysis of hydrogen peroxide with a high quantum yield of two radicals per molecule of H_2O_2. Additionally, H_2O_2 quickly decomposes to H_2O, and no hazardous by-products are generated (Gligorovski et al., 2015).

Different studies showed the effects of the application of these AOPs on both drinking and wastewater whereby dissolved organic compounds influenced the processes in terms of ·OH scavenging and UV absorption/scattering (Matilainen and Sillanpää, 2010; Oller et al., 2011; Russo et al., 2016). However, there have been a few studies of application for marine water disinfection that have high microbiological activity and most of the compounds are inorganic (Penru et al., 2012; Rincon and Pulgarin, 2004; Yamada et al., 2013). In previous studies, both UV/H_2O_2 and UV/TiO_2 have demonstrated his effectiveness in comparison with UV sole (Moreno-Andrés et al., 2016; Romero-Martínez et al., 2014; Rubio et al., 2013a; Rubio et al., 2013b), however, none of them assess the weight of salinity on disinfection processes.

The discharge limits for ballast water regarding the human health standard (BWMC, Rule D2) include both gram-negative (*E. coli* and *V. cholerae*) and a gram-positive bacteria (Intestinal *Enterococci*). It is well-known that gram-negative bacteria are more

93 sensitive to UV-based treatments than gram-positive mainly because of the differences
94 in their cell envelope (Romero-Martínez et al., 2014; Silhavy et al., 2010; van Grieken
95 et al., 2010). Moreover, it is also known that fecal enterococci can survive longer in
96 seawater than fecal coliforms (Belkin and Colwell, 2005; Byappanahalli et al., 2012). In
97 this aspect, *E. faecalis,* a typical species within an enterococci subgroup*,* was selected as
98 a microbiological indicator in this study. AOPs-disinfection studies of *E. faecalis* have
99 been developed (Lanao et al., 2012; Koivunen and Heinonen-Tanski, 2005; van Grieken
100 et al., 2010; Venieri et al., 2011; Ortega-Gómez et al., 2013), however, most of them
101 used solar UV as a source of light together with an absence of water flow, i.e., batch
102 conditions.

103 Moreover, an ideally standard test organism (STO) should be easily cultured, easy to
104 achieve high concentrations in water, and be stable over time (USEPA, 2010, 2006). In
105 addition, especially when UV-based technologies are applied, it should accord with the
106 Bunsen-Roscoe photochemical principle (Bunsen and Roscoe, 1862) which establishes
107 that the biological effect (inactivation) is directly related to the total dose of energy
108 regardless of how it has been administered, i.e., the intensity of the UV-dose should not
109 interfere with the UV-inactivation; it must reciprocate the time-dose. This principle can
110 be evaluated through a simple biodosimetry test (USEPA, 2006) which involve a batch-
111 scale testing (low UV intensity) to define a specific dose-response curve that can be
112 used for obtaining the Reduction Equivalent Dose (RED) on a continuous reactor (high
113 UV intensity). In this way, accuracy about a theoretically calculated UV-dose can be
114 obtained. It is very important because the UV-dose, unlike chemical disinfectants,
115 cannot be directly measured. Furthermore, the UV-dose is directly related with
116 disinfection efficiency (Hijnen et al., 2006). To the best of our knowledge, no published
117 work has assessed the viability of *E. faecalis* as a viable biodosimeter for UV-validation
118 purposes against other bacteria such as *E. coli* or *B. subtillis* (Li et al., 2013; Tang and
119 Sillanpää, 2015; USEPA, 2006).

120 Hence, the objectives of this research are: (i) to assess the viability of *E. faecalis* as an
121 STO in terms of obeying a time-dose reciprocity law through a biodosimetry test and
122 (ii) to evaluate the salinity as a key factor on the effectiveness of different UV-based
123 technologies in a continuous-flow reactor and asses their viability as BWTs.

124

2. Material and Methods

2.1 Water matrices

The inactivating effects of UV-based treatments were tested for organisms suspended in two water matrices with different salinity. A low salinity matrix (DW_{Buff}) was prepared with Milli-Q® (Millipore Iberica, Madrid, Spain) water by adding a phosphate-buffer solution. A high salinity matrix (SW) was prepared with 35 $g \cdot L^{-1}$ of natural marine salt (obtained by evaporation of seawater from "La Tapa" salt-works, Bahía de Cádiz, Spain) added to Milli-Ro® water. It was filtered and sterilized prior to the experiments.

Physicochemical characterization of the waters used in the experiments was performed (Table 1). Conductivity, pH at 20 ºC (Crison Multimeter MM41), and UVT_{254} transmittance (Jenway 7315 spectrophotometer) were controlled throughout all experimental procedures. A Total Organic Carbon (TOC) analysis was conducted using a Shimadzu TOC-L Analyzer with an NPOC method. Different ions were analyzed with ion chromatography (881-Compact IC Pro; 882-Compact IC Plus, Metrohm) with detection by conductivity; carbonates and bicarbonates with Titrando 905-Metrohm.

2.2 Bacterial strain and microbiological procedures

A bacterial strain of *E. faecalis* (ATCC 27285) was acquired from the Spanish Type Culture Collection (University of Valencia, Spain); following previous protocols (Moreno-Andrés et al., 2016; Romero-Martínez et al., 2014), it was preserved as 50:50 glycerol-water suspensions at -20ºC. Preserved bacteria were reactivated and then subcultured daily a maximum of three days. Culture medium (Brain and Heart Infusion Broth (Scharlab)) with bacteria in an exponential growth phase was centrifuged, and the pellets were suspended in 100 mL of buffered distilled water to obtain the bacterial inoculum to be added to the different water matrices for experimentation.

Post-treatment analysis of surviving organisms were determined by filtration through gridded membranes of 0.45 µm (Pall Corporation, NY, USA) and subsequently plated into Petri dishes with selective agar-based medium (Slanetz-Bartley Agar Base (Scharlab) with TTC indicator) according to the Membrane Filtration Method. Ten-fold dilutions were filtered from each sample in triplicate. Plates were incubated at 37 ºC for

48 hours. Colonies were counted after the incubation period, and the dilution providing between 20 and 100 colonies as the correct outcome of sample was selected.

2.3 Biodosimetry test

In order to evaluate the viability of the indicator *E. faecalis* as well as the precision of calculated UV-Dose, a simple biodosimetry test was performed in accordance with the protocol stablished in USEPA, 2006, and used for this purpose by different authors (Li et al., 2013; Sommer et al., 1995). Briefly, the bioassay is performed by using (i) a batch-scale test in which a UV-Dose-Response Curve ($D\text{-}R_{Curve}$) is defined and (ii) a dynamic test with a Continuous-flow photoreactor (CFPhr) where the log inactivation at different conditions of flow rate, UVT_{254}, and UV intensity is determined.

2.3.1 Batch-scale test

E. faecalis was exposed to a series of known doses from a collimated beam reactor (CB) that was defined and used in previous studies (Moreno-Andrés et al., 2016; Romero-Martínez et al., 2014). The light source is a UV-C low-pressure lamp (Wedeco-water solutions): electric power 10W, and UV-C efficiency was considered of 26.3% according to Bolton, 2000, and supported by actinometrical experiments (Rubio et al., 2013a; Vélez-Colmenares et al., 2011). The UV-Dose was calculated according to the protocol proposed by Bolton and validated by USEPA (Bolton and Linden, 2003; USEPA, 2006), and it was varied by changing the time of UV exposure to the inoculated matrix water. UV_{254} intensity on the sample surface was measured by a PCE-UV36 radiometer (PCE-Iberica).

2.3.2 Continuous flow test

Different assays were performed in parallel on CFPhr under the laboratory conditions defined in Moreno-Andrés et al., 2016. The CFPhr contained the same lamp and water matrix as the CB, thus the UVT_{254} and the lamp power remained constant with the flow rate being the only variable. With modifications on flow rate, the log inactivation (Log I) at the outlet was determined according to $\text{Log I} = \text{Log} (N_0/N)$, where N_0 is the initial concentration of bacteria, i.e., $CFU \cdot mL^{-1}$, before treatment and N the concentration of bacteria after treatment. Experimental operation was carried out according to Section 2.4.2 Experimental procedure.

184 *2.3.3 UV-Dose determination*

185 The Reduction Equivalent Dose, RED ($mJ \cdot cm^{-2}$), was considered by entering the Log I
186 into the D-R_{Curve} defined on the batch-scale test. The RED has been adjusted to the
187 uncertainties and biases according to USEPA, 2006. In contrast, the UV-dose on CFPhr
188 (D_{CFPhr}) was calculated as a function of Hydraulic Retention Time and mean intensity in
189 accordance with USEPA specifications as well as that applied in previous studies
190 (Moreno-Andrés et al., 2016; Romero-Martínez et al., 2014; Rubio et al., 2013a;
191 USEPA, 1986). In this way, was obtained information and accuracy about D_{CFPhr}
192 calculated theoretically.

193 ***2.4 Experimental set-up for disinfection treatment comparison***

194 *2.4.1 UV-based treatments*

195 Two different UV-continuous reactors were used for applying three different treatments:
196 UV sole; UV + TiO_2 and UV + H_2O_2.

197 An annular PVC-reactor (4.4 cm in diameter) with an irradiated volume of 510 mL was
198 utilized for UV and UV/H_2O_2 treatments. In the case of UV/H_2O_2, hydrogen peroxide
199 (30% by weight, Merck) was added in a single dosage until a concentration of 5 $mg \cdot L^{-1}$
200 was reached in the solution. It was measured prior to and after the assays according to
201 the colorimetric method and neutralized after treatment with catalase (Sigma-Aldrich).
202 A detailed methodology and optimization process was performed in previous studies
203 (Moreno-Andrés et al., 2016). Photocatalytic treatment was performed on an annular
204 TiO_2 reactor (Wallenius water AB), pH_{ZPC}=6.3; with an irradiated volume of 360 mL
205 and 3.6 cm in diameter.

206 The source of light was the same for the different reactors: low-pressure UV-C lamp
207 (electric power 42 W) equipped with a quartz sleeve (2.4 cm in diameter) which permits
208 a comparison of results. Working flow-rates (it was verified that the water in the reactor
209 remained a plug flow (Romero-Martínez et al., 2014)) were 550-3500 $L \cdot h^{-1}$ which
210 means 1.01-0.16 seconds of hydraulic retention time for a single pass.

211 *2.4.2 Experimental procedure*

The experimental premise consisted of samples treated with different UV doses that were applied on the different water matrices (DW_{Buff} or SW) and treatments (UV, UV/TiO_2, UV/H_2O_2).

The reactivated bacterial suspension was inoculated in different matrices. Inoculated matrices were stored for 30 min prior to the treatment application in order to ensure bacterial adaptation. The bacterial concentration after this acclimatization period was considered as the initial concentration in the experimental series (10^6-10^7 CFU·mL^{-1}). Meanwhile, the materials and elements of the rigs were cleaned and disinfected with hypochlorite and then rinsed with sterile water. Contamination of the elements was controlled throughout the experimentation with blank petri plates.

As indicated in Fig. 1, an inoculated water matrix was pumped in once from the storage tank (25 L.) through the continuous reactor at different flow rates and thus different UV doses were applied. To avoid the contamination of the subsequent section to the reactor, UV doses were applied in descending order. Once the flow rate was stabilized, a volume similar to the total system volume was wasted, and the sample was subsequently collected in a sterile 500 mL Erlenmeyer flask at the reactor outlet. After collecting a sample, the flow rate was increased and the process repeated again before taking a series of samples treated with different UV doses. Finally, a control for each experimental series was taken using the highest flow rate used in treated samples but after turning off the UV lamp. In that way, variations in bacterial concentration caused by pumping through the system (mechanical stress), bacterial adsorption phenomena, or changes over the course of the experiment were monitored. No significant changes were observed. Samples in the same experimental series were taken during a time lapse of 15 min maximum and stored in a cool dark recipient until microbiological analysis (Section 2.2).

2.5 Experimental design and data treatment

A multilevel factorial design was applied as a utile statistical tool for research efficiency (Álvarez-Díaz et al., 2014). Two factors were defined as experimental domain: Treatment (UV, UV/H_2O_2, UV/TiO_2) and Salinity (DW_{Buff}, SW). Six tests were stablished by triplicate resulting in 18 total runs (Table 2).

The effectiveness of disinfection was determined by logarithmic reduction of the survival microorganisms: Log (N/N_0). The different concentrations were measured in three replicates and obtaining, in all cases, a coefficient of variation less than 30%.

The obtained experimental points were modelled with a GInaFiT tool (Geeraerd et al., 2005). The goodness of fit for experimental data was evaluated through the coefficient of determination (r^2); values greater than 0.90 are considered as acceptable-fitting. It was supported with the Root Mean Square Error (RMSE) whereby two models were the most suitable for experimental data: first-order kinetic model (Eq.1) and Log-linear + shoulder (Geeraerd et al., 2000) (Eq. 2)

$$N = N_0 \cdot e^{(-k_{max} \cdot UVDose)} \quad \text{Eq. (1)}$$

$$N = N_0 \cdot \frac{e^{(-k_{max} \cdot UVDose)} \cdot e^{(k_{max} \cdot Shoulder\ Length)}}{1 + e^{(-k_{max} \cdot UVDose)} \cdot (e^{(k_{max} \cdot Shoulder\ Length)} - 1)} \quad \text{Eq. (2)}$$

Once the model was applied, two variable responses were obtained and defined for analysis: Kinetic rate constant, k_{max} ($cm^2 \cdot mJ^{-1}$) and the estimated dose necessary for decreasing the viable bacteria by ‘‘4” magnitude orders, D_4 ($mJ \cdot cm^{-2}$). It has been considered as a good disinfection goal as fecal bacteria rarely exceed 10^4 CFU·100 mL^{-1} in natural waters (Ondiviela et al., 2012), and it further permits an easy comparison of disinfection efficacy between different treatments and kinetic models. A minimum of six experimental points were fitting on the model for estimating both k_{max} and D_4.

Descriptive analysis, multifactorial analysis of the variance (ANOVA) with a 0.05 significance level, and *post-hoc* analysis with Tukey's multiple comparisons tests were performed with Statgraphics® Centurion XVII (Version 17.0.16-Statpoints Technologies, Inc.).

3. Results and discussion

The purpose of this paper is to assess the viability of different UV-based AOPs in marine water with *E. faecalis* as the microbiological indicator.

3.1 Assessment of E. faecalis as indicator

In order to assure that the *E. faecalis* met the time-dose reciprocity, two different experiments were performed under two different reactors: CB (lower UV-Intensity and large exposure times) and CFPhr (high intensities with very short times of exposure).

In small batch reactors, major conditions and photochemical processes can be controlled (Su et al., 2014). Consequently, the D-R_{Curve} was developed from CB data (Fig.2a). A typical D-R_{Curve} follows Log-linear inactivation which could be adapted with a shoulder phase at the beginning and tailing effect at the end (Geeraerd et al., 2005; USEPA, 2006). As it is microorganism-specific, it could limit the comparison by a range of UV-doses. In this way, D-R_{Curve} was defined according to the region of log-linear yield that occurs between the shoulder and the onset of tailing (USEPA, 2006). According to these criteria, the UV D-R_{Curve} of *E. faecalis* was defined as RED = 5.758 · Log I (r^2=0.9181), and it is validated for doses less than or equal to 25 $mJ \cdot cm^{-2}$.

With the intent of assessing the viability of *E. faecalis* as STO, time-dose reciprocity should be proved. This was accomplished by theoretically calculating the UV Dose on CFPhr (D_{CFPhr}) by using hydraulic retention time and mean intensity according to (USEPA, 1986). RED values were obtained by entering inactivation data acquired on CFPhr on a UV D-R_{Curve} defined in Fig. 2a. Both RED and UV-Dose- D_{CFPhr} were highly correlated (R^2=0.9362) with a slope value of 0.9658 (Fig.2b) meaning that similar inactivation rates were acquired both with RED values obtained experimentally and with the D_{CFPhr} estimated theoretically under continuous flow.

That similarity confirms that *E. faecalis* will have the same UV-inactivation under different sources of intensity. It could permit the comparison of results between conventional bench reactors and dynamic ones, i.e., with a continuous flow (Su et al., 2014; Taylor-Edmonds et al., 2015). Moreover, accuracy regarding dose determination was obtained: RED values determined experimentally fit well with the calculated dose (D_{CFPhr}).

These results suggest the viability of *E. faecalis* as STO including the adherence to the Bunsen-Roscoe photochemical law. *E. faecalis*, like *B. subtilis* (an organism commonly used as a biodosimeter) are Gram-positive bacteria. These organisms do not have the outer membrane like those that are Gram-negative. Instead, they have a thick peptidoglycan layer (30-100 nm) which contains many sub-layers that provide major protection (Silhavy et al., 2010). These differences in structure could provide more resistance to light treatments even with greater intensity (Rincon and Pulgarin, 2004); in fact, Gram-negative bacteria (*E. coli, V. cholerae* by means of Ballast Water indicators) breach the principle of Bunsen-Roscoe (Sommer et al., 1998; Taylor-Edmonds et al., 2015). Studies that are more detailed also show more sensitivity to UV-light for Gram-negative cells (Hijnen et al., 2006; Tang and Sillanpää, 2015; van Grieken et al., 2010).

3.2 Disinfection efficiency by UV-based treatments

Once *E. faecalis* met all of the criteria as an ideal STO, different UV-based technologies were assessed according to factorial design: UV, UV/H_2O_2, and UV/TiO_2 in which water composition based on salinity concentration was separated on DW_{Buff} and SW (Table 2).

Experimental results of the two studied variables are plotted in Fig. 3; they were obtained by applying the best fitting model (last column in Table 2). Inactivation raw data fit very well to a log-linear + shoulder model for UV treatment (Shoulder length approximately 4.75 $mJ \cdot cm^{-2}$). In the case of UV/H_2O_2 and UV/TiO_2, the shoulder phenomena was significantly reduced, obtaining shoulder values < 1.5 $mJ \cdot cm^{-2}$; thus the log-linear regression was the best fitting model.

k_{max} is the exponential kinetic rate constant associated with the log-linear regression. When the same kinetic model is applied, k_{max} is a useful parameter, however, when different kinetics models are to be compared, as in this study, accuracy diminishes. As an alternative, the D_4 parameter together with k_{max} were analyzed in order to assure reliable results.

In both water matrices, the highest k_{max} value was reached by a UV/TiO_2 process (DW_{Buff}-1.351 $cm^2 \cdot mJ^{-1} \pm 0.121$; SW-0.818 $cm^2 \cdot mJ^{-1} \pm 0.086$) followed by UV/$H_2O_2$. That means an improvement in efficiency for both AOPs. In comparison with the UV process, D_4 is reduced by 77.20%-DW_{Buff}, 60.49%-SW for photocatalysis, and 34.51%-

325 DW_{Buff}, 27.55%-SW for UV/H_2O_2. Those results are according to some authors, e.g.,
326 Rubio et al., 2013a, who reach a similar percentage of UV dose reduction (35%-SW) in
327 gram-positive marine bacteria by UV/TiO_2. In the case of photolysis of H_2O_2, Sun et al.,
328 2016, obtained approximately a 23% reduction for the D_4 parameter in *E. coli*.

329 The disinfection mechanisms are different between UV irradiation and AOPs. It is
330 known that the UV process induces intracellular DNA damage which means only
331 minimal damage on the cell surface (Cho et al., 2010). Otherwise, an AOP where the
332 primary action mechanism is the generation of ·OH that will react directly to the cell
333 wall, will result in oxidative damage that leads to cell death (Chong et al., 2010;
334 Pulgarin et al., 2012). This supports the improvement of disinfection efficiency for both
335 processes with an increase of k_{max} that accelerates disinfection and permits a reduction
336 of dose requirements to reach a specific disinfection goal (D_4).

337 There are several previous works in the literature regarding *E. faecalis* inactivation by
338 either UV/TiO_2 or UV/H_2O_2. This study used UV-C as a light source; regarding
339 UV/H_2O_2 process, results obtained improve those with UV_{solar} (Lanao et al., 2012;
340 Ortega-Gómez et al., 2013) because H_2O_2 absorbs radiation mainly on 100-280 nm
341 (Gligorovski et al., 2015; Lanao et al., 2012). Additionally, the use of a CFPhr that
342 results in higher UV intensity could also improve the process in terms of H_2O_2
343 photolysis and obtain major disinfection efficacy than those assays in CB reactors
344 (Koivunen and Heinonen-Tanski, 2005).

345 When photocatalysis is applied, there are two main configurations: suspended and
346 immobilized TiO_2. *E. faecalis* inactivation is generally conducted under a UV_{solar} source
347 in a slurry photo-catalytic reactor (Lanao et al., 2012; Malato et al., 2009; Venieri et al.,
348 2011) and some under immobilized TiO_2 (Fisher et al., 2013; van Grieken et al., 2010).
349 When suspended TiO_2 is applied, the process could be more effective because that
350 means a high total surface area per volume. However, it does not permit a continuous
351 operation because the catalyst suspended must be recovered (Malato et al., 2009). When
352 TiO_2 is fixed, it permits a continuous operation: a CFPhr involves high light intensity
353 that generates more radicals on a photocatalytic surface and subsequent bacteria
354 inactivation (Rincón and Pulgarin, 2003). The light wavelength could have
355 consequences on the photocatalytic reaction as well; the use of a UV-C (253.7 nm)
356 means major energy per photon (4.88 eV) that results in a higher degree of cell damage

than UV_{solar}. It could enhance the effectiveness on the photonic activation of TiO_2 (Chong et al., 2010) which is activated at a wavelength <385 nm (Rubio et al., 2013a). According to the results, it makes the process viable for these types of treatments that involve continuous operation for short treatment periods.

3.3 Salinity effects

The processes used in this study can be affected by water composition (Rincon and Pulgarin, 2004), specifically, the weight of salinity on UV-based disinfection processes is not well-defined because the photolytic mechanisms have remained ambiguous. Since salinity is a key factor for BWTs, experimental data were subjected to an ANOVA test-factorial analysis of the variance (Table 2). It will detect if there are significant differences between water matrices and if the salinity factor affects the different processes.

Results from ANOVA were summarized in Table 3. For both k_{max} and D_4, differences were detected in the results related to the Treatment factor, Salinity factor, and the interaction of both. As the interaction of both factors (treatment and salinity) is significant, they must be considered instead of the individual factors (Scheffé, 1999).

Interaction effects for both variable responses were analyzed (*Post-hoc* Tukey-HSD test) and plotted in Fig. 3-outerbox where it is shown how the salinity factor affected both k_{max} and D_4 regardless of the treatment applied.

Statistical analysis for k_{max} (Fig. 3-left) indicates a significant difference by UV/TiO_2 for both salinity and treatment efficiency, i.e., a strong k_{max} reduction is obtained by means of salinity, 39.48%, and no significant differences were detected between UV and UV/H_2O_2. Regarding the D_4 parameter (Fig. 3-right), the results are slightly different. Since UV/TiO_2 is the only process with differences in salinity, three treatment groups were statistically different. Those variations on both variable responses are explained because of the kinetic model that was applied; rate inactivation has been obtained by Shoulder + Log-linear for UV and Log-linear for AOPs. Since the D_4 prediction is within the whole kinetic, and k_{max} only takes in account the Log-linear yield, the D_4 is more accurate in this sense.

386 Nevertheless, despite the salinity affection and accuracy of variable responses, UV/TiO_2
387 is still the process with higher efficiency followed by UV/H_2O_2 and UV. In fact,
388 differences in groups are determined by UV/TiO_2.

389 When UV radiation is applied, the results suggest only minimal effects from salinity on
390 inactivation rates of *E. faecalis*. Two different forms could affect UV-inactivation in
391 seawater: a light absorption or scattering effect from dissolved organic/inorganic
392 compounds (Penru et al., 2012; Rincon and Pulgarin, 2004) and an osmotic effect on
393 bacteria (van Grieken et al., 2010). Osmotic stress on *E. faecalis* caused by salinity is
394 almost non-existent, obtaining 0.07 Log-reduction within 60 min (Moreno-Andrés et al.,
395 2016); this resistance in different environments with high ranges of salinities is known
396 (Belkin and Colwell, 2005). On the other hand, dissolved compounds could absorb light
397 causing a shielding effectiveness on bacteria obtaining lower inactivation rates as in
398 (Chen et al., 2016; Rubio et al., 2013b). In our case, the inactivation rates were slightly
399 higher in high salinity media and could be attributed to minor osmotic stress. Further,
400 the dissolved organic compounds in water are minimal (TOC= 1.816 mg $C \cdot L^{-1}$) with the
401 UVT_{254} being similar between both water matrices. In this way, the differences between
402 DW_{Buff} and SW were within the deviation for the 95% and can be considered
403 imperceptible. The same fact was obtained by Spuhler et al., 2010 as well as Agbaba et
404 al., 2016 in which no effects of water treatments on the organic compounds in the range
405 of TOC (1-4 mg $C \cdot L^{-1}$) and UV_{254} (0-0.07) were evidenced, which is within our range.

406 When AOPs are applied, the generation of ·OH radicals are involved together with the
407 effects of UV radiation on the disinfection processes and inactivation routes
408 (Gligorovski et al., 2015; Rubio et al., 2013b). As shown in Fig. 3, there are some
409 effects from salinity when AOPs are applied. D_4 increased by 5.66% on UV/H_2O_2 and
410 65.54% on UV/TiO_2 in comparison with DW_{Buff} (Table 4).

411 In SW, appear halide ions and concomitant cations that are marginally present in
412 DW_{Buff}. From the perspective of AOPs, these compounds act as scavengers of ·OH. The
413 most significant anions are Cl^- and Br^-. Cl^- is the most abundant halide in these types of
414 waters, however, Br^- is the halide of more significant concern due to the strong
415 scavenging rate together with CO_3^- (Grebel et al., 2010; Rubio et al., 2013b; Song et al.,
416 2015). In the case of SO_4^{2-}, it has an inconsequential hindering effect in comparison
417 with Cl^- (Rincon and Pulgarin, 2004; Song et al., 2015). As a result, sub-reactive species

418 appear that convert the non-selective ·OH radicals to selective radicals whereby their
419 treatment efficiency will depend on the attacking groups, i.e., nucleophiles or
420 electrophiles. Hence, the treatment efficacy is highly contaminant specific with a slow
421 reaction of sub-reactive species with electrophiles groups and highly reactive with
422 nucleophiles functional groups (Afzal et al., 2012; Grebel et al., 2010).

423 This explanation could describe the results obtained under the UV/H_2O_2 process in
424 which the efficacy of the treatment is slightly affected on the SW matrix. Although there
425 is scavenging of ·OH radicals caused by the ions, the sub-reactive species could
426 selectively react with the nucleophilic peptidoglycan substrates (Silhavy et al., 2010;
427 Sun et al., 2016) resulting in similar bacteria inactivation. Other studies have obtained
428 similar results, i.e., slight effects detected by salinity when UV/H_2O_2 is applied
429 (Pradhan et al., 2016; Rubio et al., 2013b).

430 The UV/TiO_2 process is an AOP and will have the same effect on ·OH scavenging;
431 however, the disinfection effectiveness is significantly different on SW than on
432 UV/H_2O_2. The generation of ·OH radicals is derived from light incidence on a
433 photocatalytic surface, leading to a positive electron hole (h^+_{VB}). At this point, ions
434 could have two different responses: bacterial adhesion to the photocatalytic surface and
435 ion-blockage of the active sites.

436 Counter ions, especially Ca^{2+} and Mg^{2+}, could attract bacteria to the TiO_2 catalytic
437 surface because of neutralization of repulsion forces, meaning a major bacterial
438 inactivation (Pablos et al., 2013); otherwise, the surface charge of the catalyst becomes
439 negatively charged due to the pH of both water matrices always being above pH_{ZPC}
440 (Chong et al., 2010; Rincon and Pulgarin, 2004). Our results reflect the significant
441 decrease in bacteria inactivation; this could be due to the action of scavenger ions that
442 appear to be predominant in water interaction. Additionally, when halide ions are
443 present, they can create blockage in the active sites on the photocatalytic surface and
444 reduce TiO_2 valence band holes by reacting with the generated ·OH (Bhatkhande et al.,
445 2002; Surolia et al., 2007). This effect leads to a significate decrease in rate inactivation
446 caused by the competition between anions and active sites. It may contaminate the TiO_2
447 catalyst, and the photocatalytic efficiency could diminish slowly during long-term use
448 (Linsebigler et al., 1995).

In summation, results suggest some obstruction by salinity when AOPs are applied (Table 4). In the case of UV/H_2O_2, the disinfection efficiency is less than photocatalysis, but it does not show major effects caused by salinity. While ·OH scavenging processes by ions triggered the formation of sub-reactive species, it selectively reacts with nucleophile groups, meaning a contaminant specific reaction. In terms of disinfection efficiency, salinity does not majorly interfere with the UV/H_2O_2 process. Different results appear on UV/TiO_2 in which salinity interferes most significantly in the disinfection process because of the blockage of active sites by anions' adsorption on the catalytic surface. Further studies about the possible remediation of this poisoning effect are recommended, as it is a critical issue.

Finally, the UV-based technologies assessed in this study appear to indicate that non-toxic by-products are involved (Grebel et al., 2010) because the generation of different radicals are short-lived with only a few nanoseconds of reaction (Malato et al., 2009). Additionally, they have the capacity to work with a high water-flow that is needed according to ballasting/de-ballasting rates in vessels. According to the results, it is recommended to scale-up, suggesting the potential of AOPs for the treatment of marine water instead of chemical treatments that could generate harmful by-products with associated negative impacts on sea environments (Werschkun et al., 2014).

4. Conclusions

In this laboratory study, different UV-based treatments were tested as alternatives for marine water disinfection and focused on the Ballast water global challenge. The conclusions that were drawn are shown below:

First, an assessment of the *E. faecalis* indicator shows great potential instead of other Gram-negative indicators because of the differences in cell structure. *E. faecalis* demonstrates adherence to the Bunsen-Roscoe law of time-dose reciprocity. It could allow comparing results between conventional batch reactors and dynamic photo-reactors as long as the kinetics are on the region of linear log inactivation. The results suggest *E. faecalis* as a good Standard Test Organism for seawater.

Both AOPs (UV/H_2O_2 and UV/TiO_2) have demonstrated more disinfection efficiency than UV alone even in waters with a high salinity concentration. The efficacy of the treatment increased according to $UV<UV/H_2O_2<UV/TiO_2$. Two variables responses were studied in terms of kinetic rates (k_{max}) and UV-dose reductions (D_4). When different kinetics models should be compared, results suggest the suitability of a D_4 parameter (disinfection goal) as a disinfection efficiency indicator. In this way, the accuracy of measurement could be improved in comparison with k_{max} that take in account the log-linear phase without modifications as shoulder or tailing singularities.

While little impact of salinity has been determined on the UV/H_2O_2 process, significant effects had been found mainly in UV/TiO_2 treatment. In both processes, a scavenging effect of ·OH is involved caused by halide ions, however, the ion-blockage of the active sites on a photocatalytic surface appears to be of major influence. Nevertheless, photocatalytic treatment is the process where major inactivation rates were obtained despite the salinity effect.

Acknowledgments

This research has been developed under the R+D Project AVANTE (CTM2014-52116-R) and CTQ2014-51693-REDC funded by Spanish Ministry of Economy and Competitiveness.

497 5. References

498 Afzal, A., Drzewicz, P., Martin, J.W., Gamal El-Din, M., 2012. Decomposition of
499 cyclohexanoic acid by the UV/H2O2 process under various conditions. Sci. Total
500 Environ. 426, 387–92. doi:10.1016/j.scitotenv.2012.03.019

501 Agbaba, J., Jazić, J.M., Tubić, A., Watson, M., Maletić, S., Isakovski, M.K., Dalmacija,
502 B., 2016. Oxidation of natural organic matter with processes involving O3,H2O2
503 and UV light: formation of oxidation and disinfection by-products. RSC Adv. 6,
504 86212–86219. doi:10.1039/C6RA18072H

505 Álvarez-Díaz, P.D., Ruiz, J., Arbib, Z., Barragán, J., Garrido-Pérez, C., Perales, J. a.,
506 2014. Factorial analysis of the biokinetic growth parameters and CO_2 fixation rate
507 of *Chlorella vulgaris* and *Botryococcus braunii* in wastewater and synthetic
508 medium. Desalin. Water Treat. 52, 4904–4914.
509 doi:10.1080/19443994.2013.808590

510 Belkin, S., Colwell, R.R., 2005. Oceans and Health: Pathogens in the Marine
511 Environment. Springer.

512 Bhatkhande, D.S., Pangarkar, V.G., Beenackers, A.A., 2002. Photocatalytic degradation
513 for environmental applications - a review. J. Chem. Technol. Biotechnol. 77, 102–
514 116. doi:10.1002/jctb.532

515 Bolton, J., 2000. Calculation of ultraviolet fluence rate distributions in an annular
516 reactor: significance of refraction and reflection. Water Res. 34, 3315–3324.
517 doi:10.1016/S0043-1354(00)00087-7

518 Bolton, J.R., Linden, K.G., 2003. Standardization of Methods for Fluence (UV Dose)
519 Determination in Bench-Scale UV Experiments. J. Environ. Eng. 129, 209–215.

520 Bunsen, R., Roscoe, H., 1862. Photochemische Untersuchungen. Ann Phys Chem 117,
521 529–562.

522 Byappanahalli, M.N., Nevers, M.B., Korajkic, A., Staley, Z.R., Harwood, V.J., 2012.
523 Enterococci in the Environment. Microbiol. Mol. Biol. Rev. 76, 685–706.
524 doi:10.1128/MMBR.00023-12

525 Chen, P.-Y., Chu, X.-N., Liu, L., Hu, J.-Y., 2016. Effects of salinity and temperature on
526 inactivation and repair potential of Enterococcus faecalis following medium- and

low-pressure ultraviolet irradiation. J. Appl. Microbiol. 120, 816–25. doi:10.1111/jam.13026

Cho, M., Kim, J., Kim, J.Y., Yoon, J., Kim, J.-H., 2010. Mechanisms of Escherichia coli inactivation by several disinfectants. Water Res. 44, 3410–8. doi:10.1016/j.watres.2010.03.017

Chong, M.N., Jin, B., Chow, C.W.K., Saint, C., 2010. Recent developments in photocatalytic water treatment technology: a review. Water Res. 44, 2997–3027. doi:10.1016/j.watres.2010.02.039

Cruise Market Watch, 2014. Growth of the Cruise Line Industry [WWW Document]. http://www.cruisemarketwatch.com/growth/.

Čulin, J., Mustać, B., 2015. Environmental risks associated with ballast water management systems that create disinfection by-products (DBPs). Ocean Coast. Manag. 105, 100–105. doi:10.1016/j.ocecoaman.2015.01.004

Fisher, M.B., Keane, D.A., Fernández-Ibáñez, P., Colreavy, J., Hinder, S.J., McGuigan, K.G., Pillai, S.C., 2013. Nitrogen and copper doped solar light active TiO2 photocatalysts for water decontamination. Appl. Catal. B Environ. 130, 8–13. doi:10.1016/j.apcatb.2012.10.013

Geeraerd, A.H., Herremans, C.H., Van Impe, J.F., 2000. Structural model requirements to describe microbial inactivation during a mild heat treatment. Int. J. Food Microbiol. 59, 185–209. doi:10.1016/S0168-1605(00)00362-7

Geeraerd, A.H., Valdramidis, V.P., Van Impe, J.F., 2005. GInaFiT, a freeware tool to assess non-log-linear microbial survivor curves. Int. J. Food Microbiol. 102, 95–105. doi:10.1016/j.ijfoodmicro.2004.11.038

Gligorovski, S., Strekowski, R., Barbati, S., Vione, D., 2015. Environmental Implications of Hydroxyl Radicals ((•)OH). Chem. Rev. 115, 13051–13092. doi:10.1021/cr500310b

Globallast, 2016. GloBallast [WWW Document]. The Issue. URL http://globallast.imo.org/ (accessed 9.13.16).

Grebel, J.E., Pignatello, J.J., Mitch, W.A., 2010. Effect of halide ions and carbonates on organic contaminant degradation by hydroxyl radical-based advanced oxidation

557 processes in saline waters. Environ. Sci. Technol. 44, 6822–8.
558 doi:10.1021/es1010225

559 Hijnen, W. a M., Beerendonk, E.F., Medema, G.J., 2006. Inactivation credit of UV
560 radiation for viruses, bacteria and protozoan (oo)cysts in water: a review. Water
561 Res. 40, 3–22. doi:10.1016/j.watres.2005.10.030

562 IMO, 2015. Final report on the study on the implementation of the ballast water
563 performance standard described in regulation D-2 of the BWM Convention, MEPC
564 69/4/4.

565 IMO, 2004. International Convention for the Control and Management of Ships' Ballast
566 Water and Sediments. BWM/CONF/36.

567 Koivunen, J.Ã., Heinonen-Tanski, H., 2005. Inactivation of enteric microorganisms with
568 chemical disinfectants, UV irradiation and combined chemical/UV treatments.
569 Water Res. 39, 1519–1526. doi:10.1016/j.watres.2005.01.021

570 Lanao, M., Ormad, M.P., Mosteo, R., Ovelleiro, J.L., 2012. Inactivation of
571 Enterococcus sp. by photolysis and TiO2 photocatalysis with H2O2 in natural
572 water. Sol. Energy 86, 619–625. doi:10.1016/j.solener.2011.11.007

573 Li, M., Qiang, Z., Wang, C., Bolton, J.R., Lian, J., 2013. Development of monitored
574 tunable biodosimetry for fluence validation in an ultraviolet disinfection reactor.
575 Sep. Purif. Technol. 117, 12–17. doi:10.1016/j.seppur.2013.01.021

576 Linsebigler, A.L., Linsebigler, A.L., Yates Jr, J.T., Lu, G., Lu, G., Yates, J.T., 1995.
577 Photocatalysis on TiO2 Surfaces: Principles, Mechanisms, and Selected Results.
578 Chem. Rev. 95, 735–758. doi:10.1021/cr00035a013

579 Lloyd´s Register, 2014. Understanding ballast water management Guidance for
580 shipowners and operators. Lloyd´s Regist. Mar.

581 Malato, S., Fernández-Ibáñez, P., Maldonado, M.I., Blanco, J., Gernjak, W., 2009.
582 Decontamination and disinfection of water by solar photocatalysis: Recent
583 overview and trends. Catal. Today 147, 1–59. doi:10.1016/j.cattod.2009.06.018

584 Matilainen, A., Sillanpää, M., 2010. Removal of natural organic matter from drinking
585 water by advanced oxidation processes. Chemosphere 80, 351–365.
586 doi:10.1016/j.chemosphere.2010.04.067

587 Moreno-Andrés, J., Romero-Martínez, L., Acevedo-Merino, A., Nebot, E., 2016.
588 Determining disinfection efficiency on E. faecalis in saltwater by photolysis of
589 H2O2: Implications for ballast water treatment. Chem. Eng. J. 283, 1339–1348.
590 doi:10.1016/j.cej.2015.08.079

591 Ojaveer, H., Galil, B.S., Minchin, D., Olenin, S., Amorim, A., Canning-Clode, J.,
592 Chainho, P., Copp, G.H., Gollasch, S., Jelmert, A., Lehtiniemi, M., McKenzie, C.,
593 Mikuš, J., Miossec, L., Occhipinti-Ambrogi, A., Pećarević, M., Pederson, J.,
594 Quilez-Badia, G., Wijsman, J.W.M., Zenetos, A., 2014. Ten recommendations for
595 advancing the assessment and management of non-indigenous species in marine
596 ecosystems. Mar. Policy 44, 160–165. doi:10.1016/j.marpol.2013.08.019

597 Oller, I., Malato, S., Sánchez-Pérez, J.A., 2011. Combination of Advanced Oxidation
598 Processes and biological treatments for wastewater decontamination--a review. Sci.
599 Total Environ. 409, 4141–66. doi:10.1016/j.scitotenv.2010.08.061

600 Ondiviela, B., Juanes, J.A., Gómez, A.G., Sámano, M.L., Revilla, J.A., 2012.
601 Methodological procedure for water quality management in port areas at the EU
602 level. Ecol. Indic. 13, 117–128. doi:10.1016/j.ecolind.2011.05.018

603 Ortega-Gómez, E., Esteban García, B., Ballesteros Martín, M.M., Fernández Ibáñez, P.,
604 Sánchez Pérez, J. a., 2013. Inactivation of Enterococcus faecalis in simulated
605 wastewater treatment plant effluent by solar photo-Fenton at initial neutral pH.
606 Catal. Today 209, 195–200. doi:10.1016/j.cattod.2013.03.001

607 Pablos, C., van Grieken, R., Marugán, J., Chowdhury, I., Walker, S.L., 2013. Study of
608 bacterial adhesion onto immobilized TiO2: Effect on the photocatalytic activity for
609 disinfection applications. Catal. Today 209, 140–146.
610 doi:10.1016/j.cattod.2012.12.010

611 Penru, Y., Guastalli, A.R., Esplugas, S., Baig, S., 2012. Application of UV and
612 UV/H2O2 to seawater: Disinfection and natural organic matter removal. J.
613 Photochem. Photobiol. A Chem. 233, 40–45.

614 Pradhan, S., Fan, L., Roddick, F.A., Shahsavari, E., Ball, A.S., 2016. Impact of salinity
615 on organic matter and nitrogen removal from a municipal wastewater RO
616 concentrate using biologically activated carbon coupled with UV/H2O2. Water

Res. 94, 103–110. doi:10.1016/j.watres.2016.02.046

Pulgarin, C., Kiwi, J., Nadtochenko, V., 2012. Mechanism of photocatalytic bacterial inactivation on TiO2 films involving cell-wall damage and lysis. Appl. Catal. B Environ. 128, 179–183. doi:10.1016/j.apcatb.2012.01.036

Rincon, A.G., Pulgarin, C., 2004. Effect of pH, inorganic ions, organic matter and H2O2 on E. coli K12 photocatalytic inactivation by TiO2 implications in solar water disinfection. Appl. Catal. B Environ. 51, 283–302. doi:10.1016/j.apcatb.2004.03.007

Rincón, A.G., Pulgarin, C., 2003. Photocatalytical inactivation of E. coli: effect of (continuous–intermittent) light intensity and of (suspended–fixed) TiO2 concentration. Appl. Catal. B Environ. 44, 263–284. doi:10.1016/S0926-3373(03)00076-6

Rivas-Hermann, R., Köhler, J., Scheepens, A.E., 2015. Innovation in product and services in the shipping retrofit industry: a case study of ballast water treatment systems. J. Clean. Prod. 106, 443–454. doi:10.1016/j.jclepro.2014.06.062

Romero-Martínez, L., Moreno-Andrés, J., Acevedo-Merino, A., Nebot, E., 2014. Improvement of ballast water disinfection using a photocatalytic (UV-C + TiO 2) flow-through reactor for saltwater treatment. J. Chem. Technol. Biotechnol. 1203–1210. doi:10.1002/jctb.4385

Rubio, D., Casanueva, J.F., Nebot, E., 2013a. Improving UV seawater disinfection with immobilized TiO2: Study of the viability of photocatalysis (UV254/TiO2) as seawater disinfection technology. J. Photochem. Photobiol. A Chem. 271, 16–23. doi:10.1016/j.jphotochem.2013.08.002

Rubio, D., Nebot, E., Casanueva, J.F., Pulgarin, C., 2013b. Comparative effect of simulated solar light, UV, UV/H2O2 and photo-Fenton treatment (UV-Vis/H2O2/Fe2+,3+) in the Escherichia coli inactivation in artificial seawater. Water Res. 47, 6367–79. doi:10.1016/j.watres.2013.08.006

Russo, D., Spasiano, D., Vaccaro, M., Cochran, K.H., Richardson, S.D., Andreozzi, R., Puma, G.L., Reis, N.M., Marotta, R., 2016. Investigation on the removal of the major cocaine metabolite (benzoylecgonine) inwater matrices by UV254/H2O2

process by using a flow microcapillary film array photoreactor as an efficient experimental tool. Water Res. 89, 375–383. doi:10.1016/j.watres.2015.11.059

Scheffé, H., 1999. The analysis of variance. Wiley-Interscience Publication.

Silhavy, T.J., Kahne, D., Walker, S., 2010. The bacterial cell envelope. Cold Spring Harb. Perspect. Biol. 2, 16. doi:10.1101/cshperspect.a000414

Sommer, R., Cabaj, A., Schoenen, D., Gebel, J., Kolch, A., Havelaar, A.H., Schets, F.M., 1995. Comparison of three laboratory devices for UV-inactivation of microorganisms. Water Sci. Technol. 31.

Sommer, R., Haider, T., Cabaj, A., Pribil, W., Lhotsky, M., 1998. Time dose reciprocity in UV disinfection of water. Water Sci. Technol. 38, 145–150. doi:10.1016/S0273-1223(98)00816-6

Song, C., Wang, L., Ren, J., Lv, B., Sun, Z., Yan, J., Li, X., Liu, J., 2015. Comparative study of diethyl phthalate degradation by UV/H2O2 and UV/TiO2: kinetics, mechanism, and effects of operational parameters. Environ. Sci. Pollut. Res. Int. doi:10.1007/s11356-015-5481-8

Spuhler, D., Andrés Rengifo-Herrera, J., Pulgarin, C., 2010. The effect of Fe2+, Fe3+, H2O2 and the photo-Fenton reagent at near neutral pH on the solar disinfection (SODIS) at low temperatures of water containing Escherichia coli K12. Appl. Catal. B Environ. 96, 126–141. doi:10.1016/j.apcatb.2010.02.010

Su, Y., Straathof, N.J.W., Hessel, V., Noël, T., 2014. Photochemical Transformations Accelerated in Continuous-Flow Reactors: Basic Concepts and Applications. Chem. - A Eur. J. 20, 10562–10589. doi:10.1002/chem.201400283

Sun, P., Tyree, C., Huang, C.-H., 2016. Inactivation of E. coli, Bacteriophage MS2 and Bacillus Spores under UV/H2O2 and UV/Peroxydisulfate Advanced Disinfection Conditions. Environ. Sci. Technol. acs.est.5b06097. doi:10.1021/acs.est.5b06097

Surolia, P.K., Tayade, R.J., Jasra, R. V, 2007. Effect of Anions on the Photocatalytic Activity of Fe (III) Salts Impregnated TiO2. Ind. Eng. Chem. Res. 6196–6203. doi:10.1021/ie0702678

Tang, W.Z., Sillanpää, M., 2015. Bacteria sensitivity index of UV disinfection of bacteria with shoulder effect. J. Environ. Chem. Eng. 3, 2588–2596.

677 doi:10.1016/j.jece.2015.09.010

678 Taylor-Edmonds, L., Lichi, T., Rotstein-Mayer, A., Mamane, H., 2015. The impact of
679 dose, irradiance and growth conditions on *Aspergillus niger* (renamed *A.*
680 *brasiliensis*) spores low-pressure (LP) UV inactivation. J. Environ. Sci. Heal. Part
681 A 50, 341–347. doi:10.1080/10934529.2015.987519

682 USEPA, 2010. Generic Protocol for the Verification of Ballast Water Treatment
683 Technology, Report number EPA/600/R-10/146.

684 USEPA, 2006. Ultraviolet Disinfection Guidance Manual for the Final Long Term 2
685 Enhanced Surface Water Treatment Rule., EPA 815-R-06-007. Office of Water
686 (4601), Washington, DC.

687 USEPA, 1986. Design Manual: Municipal Wastewater Disinfection. EPA/625/1-86/021.

688 van Grieken, R., Marugán, J., Pablos, C., Furones, L., López, A., 2010. Comparison
689 between the photocatalytic inactivation of Gram-positive E. faecalis and Gram-
690 negative E. coli faecal contamination indicator microorganisms. Appl. Catal. B
691 Environ. 100, 212–220. doi:10.1016/j.apcatb.2010.07.034

692 Vélez-Colmenares, J.J., Acevedo, A., Nebot, E., 2011. Effect of recirculation and initial
693 concentration of microorganisms on the disinfection kinetics of Escherichia coli.
694 Desalination 280, 20–26. doi:10.1016/j.desal.2011.06.041

695 Venieri, D., Chatzisymeon, E., Gonzalo, M.S., Rosal, R., Mantzavinos, D., 2011.
696 Inactivation of Enterococcus faecalis by TiO2-mediated UV and solar irradiation in
697 water and wastewater: culture techniques never say the whole truth. Photochem.
698 Photobiol. Sci. 10, 1744–50. doi:10.1039/c1pp05198a

699 Werschkun, B., Banerji, S., Basurko, O.C., David, M., Fuhr, F., Gollasch, S., Grummt,
700 T., Haarich, M., Jha, A.N., Kacan, S., Kehrer, A., Linders, J., Mesbahi, E., Pughiuc,
701 D., Richardson, S.D., Schwarz-Schulz, B., Shah, A., Theobald, N., von Gunten, U.,
702 Wieck, S., Höfer, T., 2014. Emerging risks from ballast water treatment: The run-
703 up to the International Ballast Water Management Convention. Chemosphere 112,
704 256–266. doi:10.1016/j.chemosphere.2014.03.135

705 Werschkun, B., Sommer, Y., Banerji, S., 2012. Disinfection by-products in ballast water
706 treatment: an evaluation of regulatory data. Water Res. 46, 4884–901.

707 doi:10.1016/j.watres.2012.05.034
708 Yamada, N., Suzumura, M., Koiwa, F., Negishi, N., 2013. Differences in elimination
709 efficiencies of Escherichia coli in freshwater and seawater as a result of TiO2
710 photocatalysis. Water Res. 47, 2770–2776. doi:10.1016/j.watres.2013.02.023
711
712
713

6. Figures and Tables

Fig. 1. Schematic of experimental procedure.

Fig. 2.a) *E. faecalis* UV Dose-Response curve (D-R_{curve}) defined as UV Dose ($mJ \cdot cm^{-2}$) Versus Log (N_0/N). In the outer box appears full kinetics for CB according to Log-linear + Tail (Log (N/N_0) is referred to microbial survival). **b)** RED values (obtained experimentally by biodosimetry test) Versus Calculated UV Dose on CFPhr (D_{CFPhr}).

Fig. 3. Descriptive plots for the two variables studied: Left – k_{max} ($cm^{-2} \cdot mJ^{-1}$). Right- D_4 parameter ($mJ \cdot cm^{-2}$). Error bars depict the 95% confidence interval. Asterisks (*) show data for differences ($p<0.05$) between water matrices (DW_{Buff}-SW) in the same treatment. Letters show differences ($p<0.05$) between treatments at DW_{Buff} (A-B) or SW (a-c). Values were obtained by an application of different kinetic models (Log-Linear + Shoulder for UV and, Log-Linear for UV/H_2O_2 and UV/TiO_2). Outer boxes show interaction effects plot for k_{max} (Left side) and D_4 (Right side).

728 **Table 1.** Characterization of water matrices used in the experimentation.

Parameter	Low Salinity matrix (DW_{Buff})	High Salinity matrix (SW)
pH	7.58 ± 0.14	8.74 ± 0.05
Conductivity at 20ºC ($\mu S \cdot cm^{-1}$)	79.06 ± 1.17	45680 ± 1493.3
Temperature (ºC)	23.83 ± 2.11	21.23 ± 2.15
UVT_{254} (%)	89.80 ± 1.84	88.28 ± 2.74
Total Organic Carbon (TOC) (mg $C \cdot L^{-1}$)	--	1.816 ± 0.049
Cl^- ($g \cdot L^{-1}$)	--	17.330 ± 0.099
SO_4^{2-} ($g \cdot L^{-1}$)	--	0.522 ± 0.008
Br^- ($mg \cdot L^{-1}$)	--	< 0.0001
Na^+ ($g \cdot L^{-1}$)	--	11.619 ± 0.145
K^+ ($mg \cdot L^{-1}$)	--	51.55 ± 2.45
Ca^{2+} ($mg \cdot L^{-1}$)	--	79.80 ± 2.60
Mg^{2+} ($mg \cdot L^{-1}$)	--	40.47 ± 0.72
CO_3^{2-} ($\mu mol \cdot L^{-1}$)	--	0.52 ± 0.10
HCO_3^- ($\mu mol \cdot L^{-1}$)	--	96.60 ± 0.20

729

730

731

732

733

734

735 **Table 2.** Experimental domain for the variables responses studied: $\mathbf{k_{max}}$ ($cm^2 \cdot mJ^{-1}$) and
736 D_4 ($mJ \cdot cm^{-2}$). They are summarized together with regression coefficient and models
737 applied for all factorial runs.

Run	*Salinity*	*Treatment*	k_{max} *($cm^2 \cdot mJ^{-1}$)*	*D4 ($mJ \cdot cm^{-2}$)*	r^2	*Kinetic Model applied*
1	DW_{Buff}	UV-C	0.351	29.12	0.962	*Log-Linear + Shoulder*
2	DW_{Buff}	UV/H_2O_2	0.489	19.05	0.904	*Log-Linear*
3	DW_{Buff}	UV/TiO_2	1.380	6.72	0.904	*Log-Linear*
4	SW	UV-C	0.435	28.8	0.944	*Log-Linear + Shoulder*
5	SW	UV/H_2O_2	0.421	22.15	0.995	*Log-Linear*
6	SW	UV/TiO_2	0.880	10.63	0.976	*Log-Linear*
7	DW_{Buff}	UV-C	0.336	31.05	0.923	*Log-Linear + Shoulder*
8	DW_{Buff}	UV/H_2O_2	0.435	21.33	0.951	*Log-Linear*
9	DW_{Buff}	UV/TiO_2	1.219	7.59	0.962	*Log-Linear*
10	SW	UV-C	0.363	29.19	0.967	*Log-Linear + Shoulder*
11	SW	UV/H_2O_2	0.474	19.46	0.966	*Log-Linear*
12	SW	UV/TiO_2	0.720	12.87	0.985	*Log-Linear*
13	DW_{Buff}	UV-C	0.359	30.74	0.921	*Log-Linear + Shoulder*
14	DW_{Buff}	UV/H_2O_2	0.484	19.15	0.918	*Log-Linear*
15	DW_{Buff}	UV/TiO_2	1.455	6.41	0.898	*Log-Linear*
16	SW	UV-C	0.419	28.83	0.985	*Log-Linear + Shoulder*
17	SW	UV/H_2O_2	0.439	21.29	0.938	*Log-Linear*
18	SW	UV/TiO_2	0.854	10.8	0.931	*Log-Linear*

738

739

740

741

742

743

744

Table 3. Summary table of ANOVA test. Significant factors at p-values under 0.05 are denoted in bold.

Variable	Factor	Degrees of freedom	Sum of Squares	Mean Square	F-value	P-value
k_{max}	**A: Treatment**	**2**	**1.802**	**0.901**	**215.400**	**<0.0001**
	B: Salinity	**1**	**0.126**	**0.126**	**30.010**	**0.0001**
	AB	**2**	**0.307**	**0.153**	**36.700**	**<0.0001**
	Error	12	0.050	0.004		
	Total	17	2.284			
D4	**A: Treatment**	**2**	**1258.890**	**629.443**	**572.360**	**<0.0001**
	B: Salinity	**1**	**9.188**	**9.188**	**8.350**	**0.0136**
	AB	**2**	**26.229**	**13.115**	**11.930**	**0.0014**
	Error	12	13.197	1.099		
	Total	17	1307.500			

759 **Table 4.** Summary table with efficiencies related to k_{max} and D_4 obtained on SW in
760 comparison with DW_{Buff} by means of salinity effects.

Treatment	k_{max} ($cm^2 \cdot mJ^{-1}$)	D_4 ($mJ \cdot cm^{-2}$)	Key findings
UV-C	16.21%	-4.50%	No significant effects have been detected. A minimal increase on efficiency could be attained to slightly osmotic stress.
UV/H_2O_2	-5.22%	5.66%	Slightly affection by salinity has been reported. The main reason is attained to scavenging rate of ·OH and consequent generation of sub-reactive species that can selectively react with bacteria.
UV/TiO_2	-39.48%	65.54%	Significant differences have been reported. Ion blockage of active sites on the catalytic surface seems to be the major effect caused by salinity.

761

Figure 1

Click here to download high resolution image

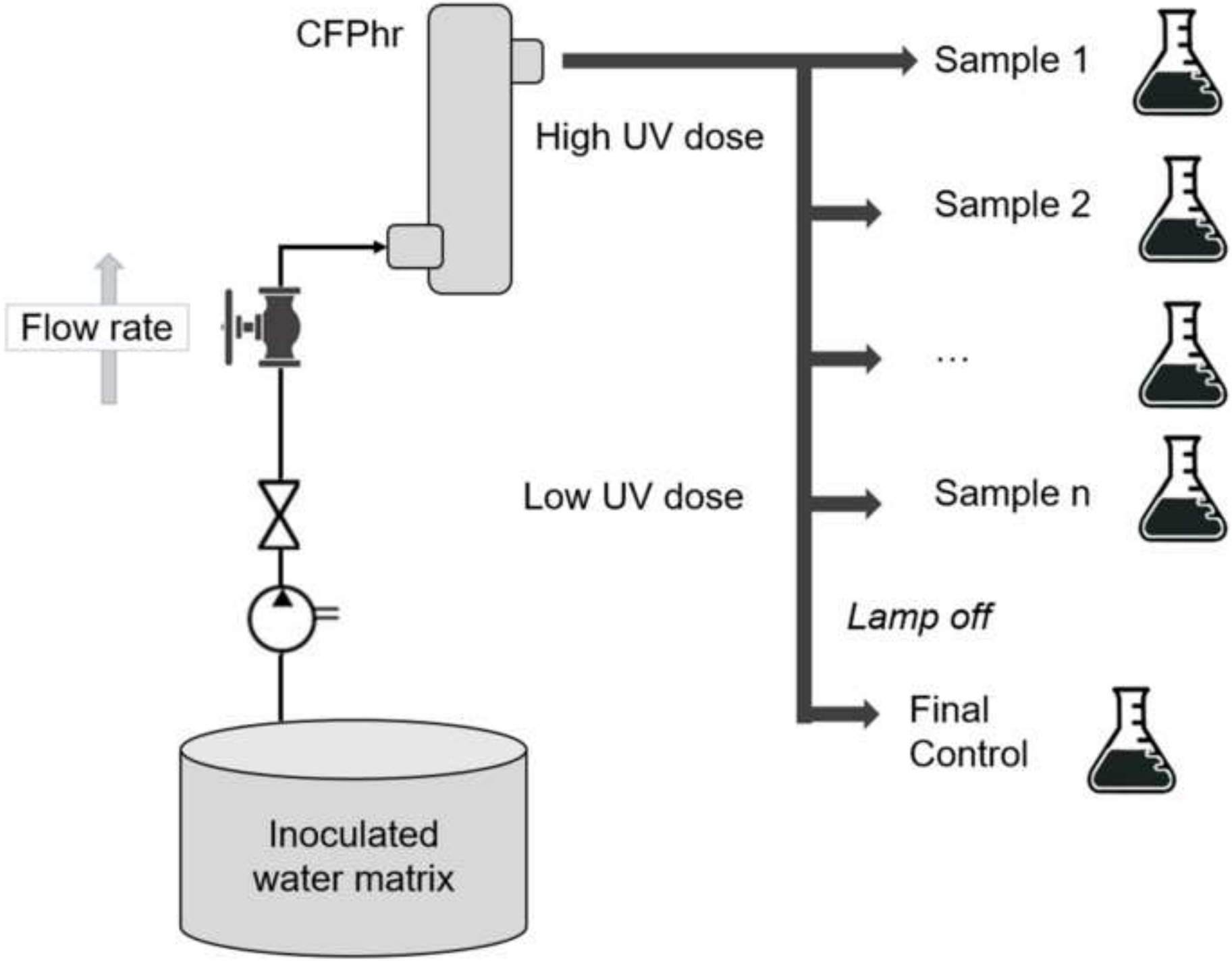

Figure 2

Click here to download high resolution image

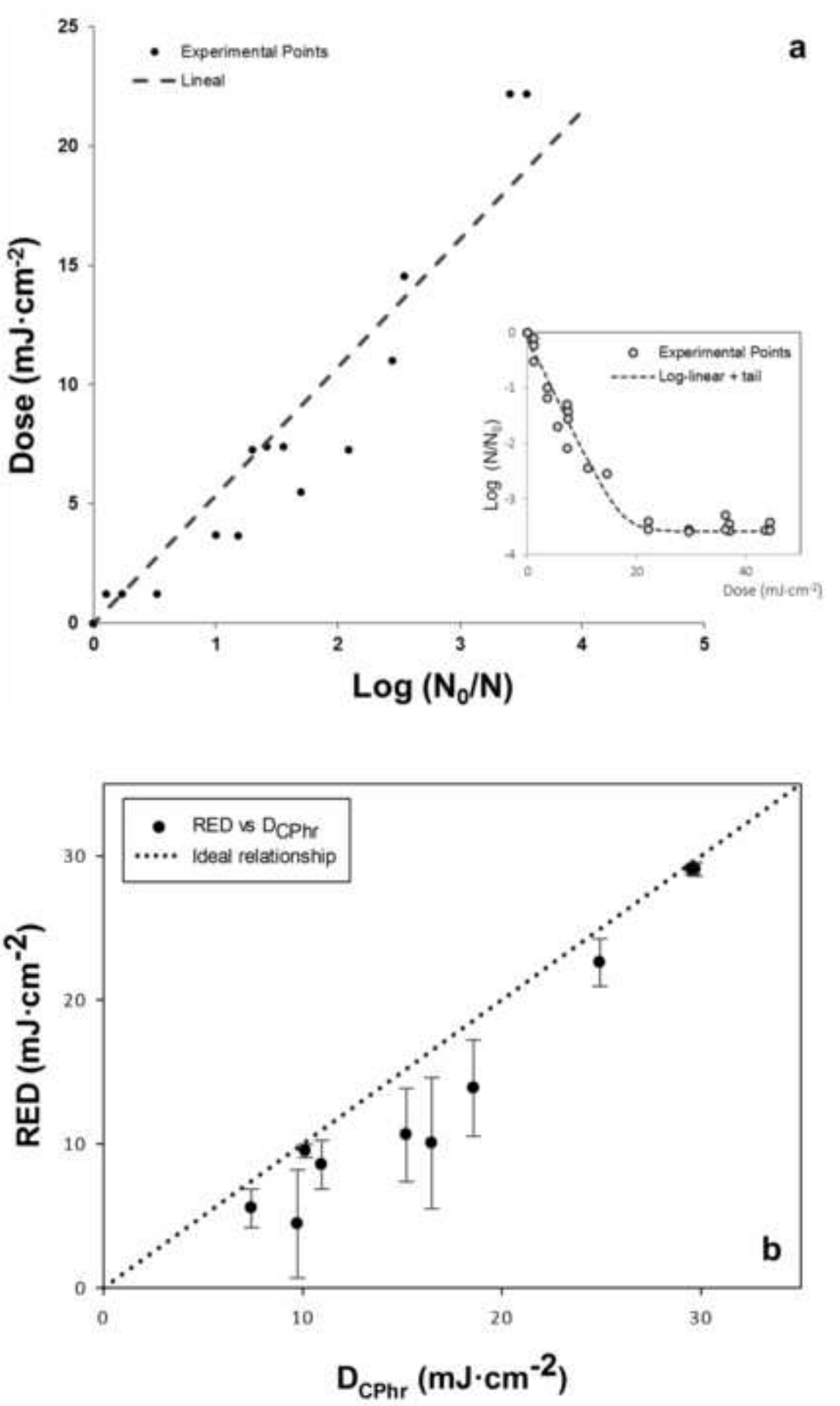

Figure 3

Click here to download high resolution image